Evaluation of Loadings in Head-Cervical-Thoracic Region for a Parameterized Aircraft Seat Backrest with Different Headrest Designs

Xianzhi Zhong[1], Yuezhi Liu[1], Obidah Alawneh[1], Reza Faieghi[1], Fengfeng Xi[1]

[1] Ryerson University, Canada

ABSTRACT

The contact loading and pressure distribution on the back are important measures to assess the comfort of a seat's backrest. On the other hand, the backrest design also influences the pressure on the back. Limited studies show how the variation on the backrest affects the loadings to the back surface, especially for the upper trunk region of the human body. In this study, a parameterized backrest model with the back support and headrest combined is created to describe design variations with different headrests. This study uses a 3D multibody model to evaluate the loadings and predict the pressure to analyze the headrest design's influences on the loading and pressure within the head-cervical-thoracic region. As a result, the headrest variation based on the parameterized model impacts the supportive load on the head. Within the thoracic region, the upper part is more sensitive to the change of design and sitting condition than the lower part. Different designs also affect the location of higher-pressure areas. The pros and cons of the analyzed designs are discussed. This study provides an example of assessing the design using the proposed load and pressure prediction method for the backrest.

KEYWORDS

Seat comfort, headrest, backrest, biomechanical model, pressure distribution, loadings

Introduction

The comfort of aircraft seats plays a critical role in the onboard experience, and improved seating comfort is a critical component that many seat manufacturers consider. One important measure for the quantification of static seating comfort/discomfort is the interaction loadings on the backrest, which is usually presented as the pressure distribution. Different methods were proposed to evaluate the pressure on the seat cushion, such as experiment-based prototype measurements, utilization of finite element model(Du et al., 2013; Paul et al., 2012), and multibody biomechanics (Cappetti & DI Manso, 2020; Liu et al., 2021). To find the pressure distribution, the backrest cushion, aside from the human model, is also an essential factor, which motivates various designs or innovations regarding cushion material and surface geometry(Franz et al., 2012; Smulders et al., 2019). However, the research that studies how different backrest designs affect the pressure distribution mainly focuses on the lower back region(Lim et al., 2000; Makhsous et al., 2009). The studies focusing on the interaction between the upper trunk and the backrest design are insufficient. This paper uses a spatial multibody model to simulate the interested head-cervical-thoracic region of the body and calculate the interaction loadings with different types of the backrest. This paper defines the backrest as a simplified parameterized model, which allows simple design variation by changing parameter values. As this is an initial study, the analyzed design variations only include the changed dimension of the headrest, which behaves as part of the seat backrest in the created backrest model.

Parameterized Design

There usually is more room and flexibility for each seat for business aircraft, the design or condition of which in this paper is simplified as a parameterized model as shown in figure 1. The five main labeled parameters describe the dimensions of the components and the surface feature of the backrest cushion. The surface geometry is presented by a surface polynomial equation referring to the cushion's body frame of x-y-z, whose origin is located at the cushion surface's mid-bottom line. The degrees of the equation may vary according to the complexity of the surface geometry. In this paper, a flat cushion surface is assumed. Therefore, the surface equation is simply $x = 0$. Due to the multiple parameters introduced, numerous designs may be generated. As an initial study, this paper only analyses two cases by varying the parameter related to the headrest, as shown in Figures 1(a) and (b). The design parameters and their values are listed in Table 1. The values are estimated respecting the SAE anthropometry data (Harrison & M, 2002) and aircraft seat design standards.

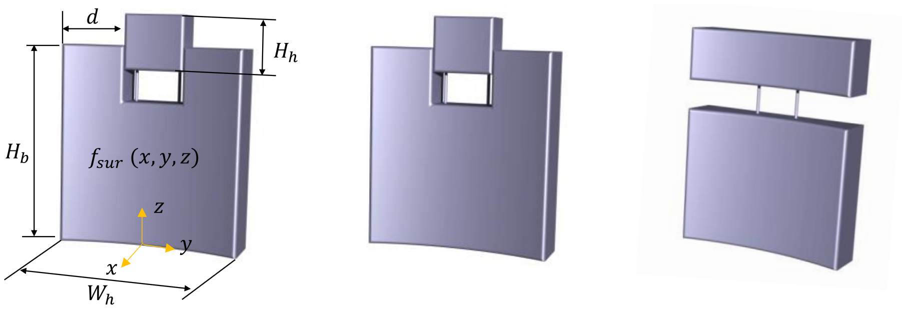

(a) (b) (c)

Figure 1: (a) Parameterized backrest with parameters labelled (b) Type A with deployed headrest (c) Type B with deployed headrest

Table 1: Backrest parameters and their values

Design parameters	**Acronyms**	**Type A**	**Type B**
Headrest offset	d	0.15 m	0 m
Headrest height	H_h	0.18 m	
Backrest height	H_b	0.652 m	
Surface shape	f_{sur}	$x = 0$	
Backrest width	W_h	0.5 m	

Modeling of Sitting

The shape of the spine dominates the posture of the upper body. The region from the head to the level of T12 is modeled with eight segments connected by spherical joints. The joint locations take the reference of the head's center of gravity and locations of intervertebral discs. Three static relaxed postures under the backrest recline angle(θ_{br}) of 30deg, 40deg, and 50deg from the vertical direction were considered for the analysis. The body inclination in the sagittal plane is determined by the trunk vector that points from Ischial Tuberosity (IT) to the joint of the C7-T1 disc. The included angle between the vector and the vertical line on the sagittal plane is named trunk inclination angle (θ_T), which is approximated to the backrest recline angle. Constrained by θ_T, the new location of the spine can be obtained by varying the joint angles within the thoracolumbar region. The change of rotation angle from a slouched initial posture (Kitazaki & Griffin, 1997) is based on interpolation referring to the range of motion data (White & Panjabi, 1990) of each intervertebral disc. The slouched posture was selected as it is considered the most relaxed initial condition. Table 2 collects the joints' coordinates that define the spine shape under different postures referring to the global frame of X-Y-Z at IT.

Table 2: Joint locations of head-cervical-thoracic segment model at different recline angles

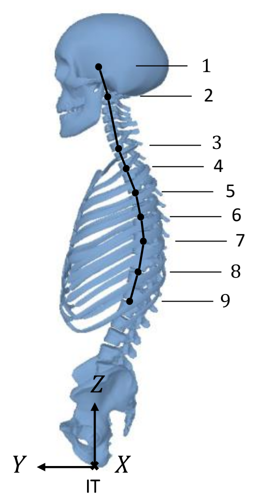

Joint	Location	$\theta_T = \theta_{br} = 30°$	$\theta_T = \theta_{br} = 40°$	$\theta_T = \theta_{br} = 50°$
1	Head (CG)	(0, -0.362, 0.687)	(0, -0.483, 0.617)	(0, -0.589, 0.527)
2	C1-C2 disc	(0, -0.382, 0.630)	(0, -0.491, 0.557)	(0, -0.583, 0.466)
3	C7-T1 disc	(0, -0.345, 0.518)	(0, -0.431, 0.456)	(0, -0.503, 0.380)
4	T2-T3 disc	(0, -0.332, 0.478)	(0, -0.409, 0.420)	(0, -0.474, 0.350)
5	T4-T5 disc	(0, -0.319, 0.438)	(0, -0.388, 0.383)	(0, -0.446, 0.318)
6	T6-T7 disc	(0, -0.305, 0.395)	(0, -0.365, 0.344)	(0, -0.416, 0.284)
7	T8-T9 disc	(0, -0.286, 0.349)	(0, -0.338, 0.303)	(0, -0.381, 0.249)
8	T10-T11 disc	(0, -0.260, 0.302)	(0, -0.303, 0.261)	(0, -0.339, 0.215)
9	T12-L1 disc	(0, -0.224, 0.248)	(0, -0.258, 0.215)	(0, -0.286, 0.178)

The condition of the analysis is static. The loadings on each body segment can then be calculated by using the recursive method going inferiorly. The region between C1 and T2 is bridged. It has no contact with the cushion under all analyzed conditions due to the lordotic curving of the cervical spine and the flatness of the analyzed backrest. Six contact points were considered for each of the other inferior segments supported by the backrest. The contact points are at the half segment length (l_i) and in width, they are evenly located along the width of the contact region at the same level (w_i). The contact region is based on the measurement of a pressure mat on a relatively flat backrest cushion. The contact points also have an approximately equal offset (d_i) from the spinal vertebra, whose value can be related to the vertebral level and trunk length (Drerup & Hierholzer, 1994). Therefore, the contact point locations for both sides can be expressed in the local frame as $\left(\pm\frac{ew_i}{14}, -d_i, \frac{l_i}{2}\right)$, where $e = 1{,}3{,}5$. The force direction is along the cushion surface's normal at the contact point location. Since the analyzed backrest is flat, the direction is defined by $(0, \cos\theta_{br}, \sin\theta_{br})$ referring to the global frame. The described condition is illustrated in figure 2. Then, the static loadings on segment i can be found by solving equations (1) and (2) based on force and moment equilibrium.

$$\boldsymbol{M}_{i+1} + \boldsymbol{l}_i \times \boldsymbol{F}_{i+1} + \frac{\boldsymbol{l}_i}{2} \times \boldsymbol{G}_i + \sum_{j=1}^{n}(\boldsymbol{c}_{ij} \times \boldsymbol{N}_{ij}) = k\boldsymbol{M}_i \quad (1)$$

$$\boldsymbol{F}_{i+1} + \boldsymbol{G}_i + \sum_{j=1}^{n} \boldsymbol{N}_{ij} = \boldsymbol{F}_i \quad (2)$$

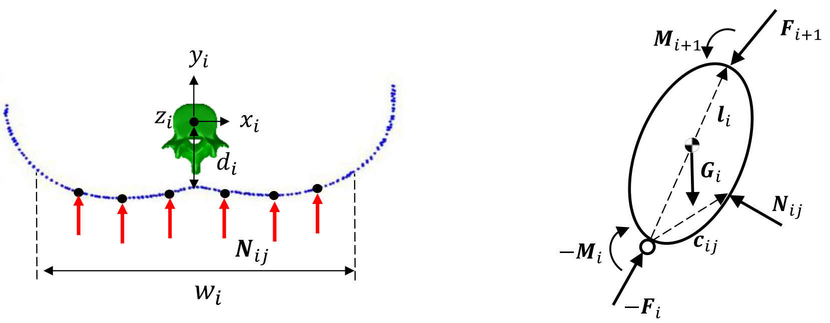

(a) (b)

Figure 2: (a) the loading condition of a fully contact trunk segment on the transverse plane (b) loads on i^{th} body segment

In equations (1) and (2), the bolded letters represent spatial vectors. $\boldsymbol{G}$ is the gravitational force; $\boldsymbol{F}$ is the load on the joint; $\boldsymbol{N}$ is the force from the backrest acting on the body of the segment; $\boldsymbol{M}$ is the joint moment from the muscle; $\boldsymbol{l}$ is the segment length vector, and $\boldsymbol{c}$ represents the vector pointing from the bottom joint to the contact point location. n is the number of the contact point on segment i. $k = 1$ when segment i is not supported, and the term $\sum_{j=1}^{n}(\boldsymbol{c}_{ij} \times \boldsymbol{N}_{ij})$ becomes zero as there is no external force. When there is an external force(s) that balances the segment, the required internal moment at the bottom joint ($\boldsymbol{M_i}$) becomes zero and therefore $k = 0$. The applied gravitational force of each segment is obtained based on the percentile weight data(Pearsall et al., 1996), which is collected in table 3. The weight and height of the analyzed body are 165cm and 72kg, respectively, based on the measurement of a subject. The considered weight ratios of segment T1-T2, T3-T4 are less than the data from literature because the arm is supported while seated. So, only half of the superior limb's weight is assumed to load on the trunk. The external forces at the assigned contact points on one side of the back are considered to have the same magnitude. In this way, the loadings of each segment can be solved determinately using equilibrium equations. With the obtained external forces and their locations on the backrest cushion and the back surface point cloud of the subject, the pressure distribution can then be simulated based on the method by Liu et al. (Liu et al., 2021).

Table 3: Percentile weights of the analyzed body segments

Segment	Considered segment weight/Total body mass
Head-C1	0.058
C2-C7	0.022
T1-T2	0.022
T3-T4	0.066
T5-T6	0.046
T7-T8	0.029
T9-T10	0.036
T11-T12	0.046

Results and Discussion

The backrest cushion's bottom line aligns to the spinal S1 level, and then the lower edge of the headrest aligns to the T3-T4 segment. Therefore, the headrest design variation only affects whether there is contact at the specific location above joint 5 (table 2). The gap under the headrest for type A is only at the center area; thus, the forces at the four contact points close to the midline are neglected, and only the two at the side exert forces (figure 2a) on the T3-T4 segment. For type B, since the headrest is across the width of the backrest, no force is exerted on the same segment. With the conditions determined, the contact loads can then be calculated. Figure 3 shows that Type A provides more support in the thoracic region but requires less support to the head compared to the case for type B. That is because the deployed headrest in type B leaves a wide gap, so the body segment weight within the gapped region generates additional moments onto the joint below. Therefore, the load on the head required to balance the moment is greater for the case of type B. Besides, type A is found to have a larger load in the Upper Thoracic (UT) region (T3-T8) because type A is not entirely gapped in the upper area. Thus, there is more contact area providing support within the region. This is also clearly revealed by the simulation of the pressure distribution (figure 4); additional contact areas in the upper region can be observed in the simulation for type A. The load and contact pressure increase in general when the backrest reclines deeper as more weight is projected onto the backrest surface. However, the loadings on the Lower Thoracic (LT) region (T9-T12) are retaining against the variation of the analyzed design and backrest recline angle. One possible reason behind this is that the applied biomechanical model assumes rigid bodies, which deviation from the actual human body made of layers of soft biological tissues. However, it can still be concluded that the recline angle does not affect the LT loading as much as that of the UT.

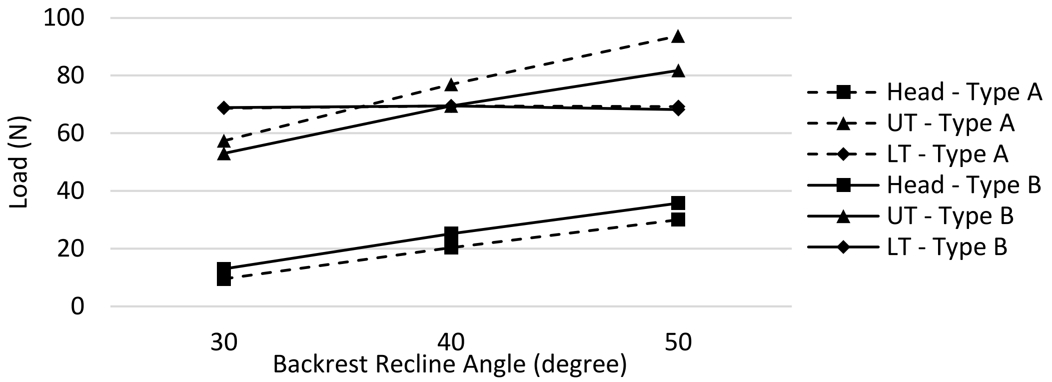

Figure 3: Loads at different regions vs. backrest recline angle for both type A and type B design

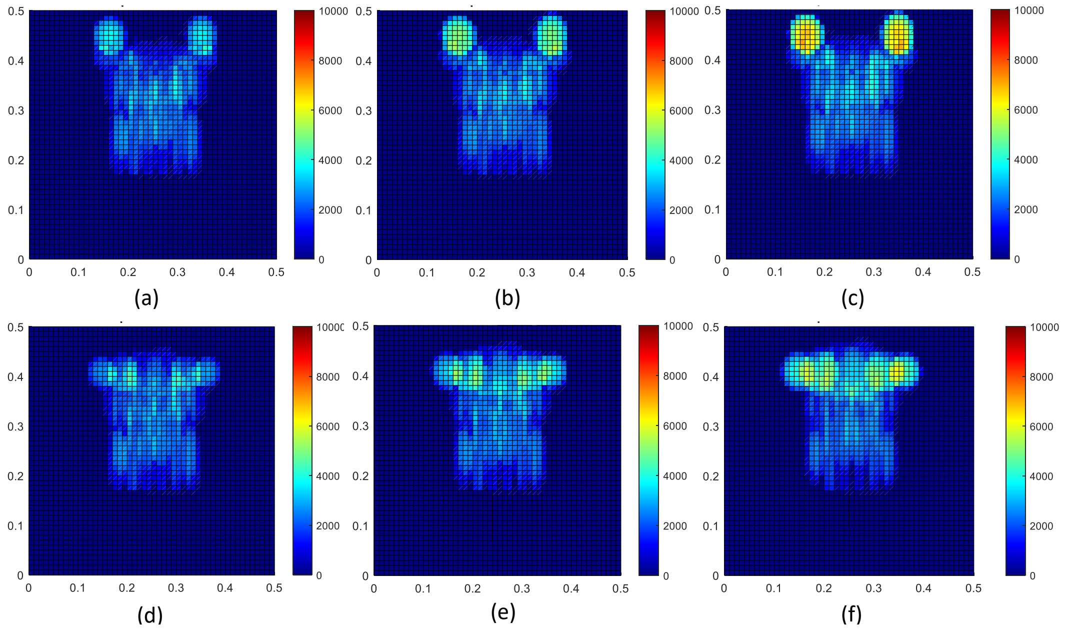

Figure 4: Simulation of the pressure distribution (Pa) in the thoracic region with type A at the recline angle of (a) 30 degree, (b) 40 degree, (c) 50 degree, and with type B (d) 30 degree, (e) 40 degree, (f) 50 degree

From figure 4, Type A is observed having the stresses peaking at the sides of the notch, and stresses are more evenly distributed in the region below. For type B, there is no notch, and the stresses concentrate around the upper edge of the backrest with a slightly lower magnitude compared to the peak pressure of type A. Although type A provides more contact area, the high-stress region is more centered separately on two sides of the upper body, which may round the shoulder and form a restrained posture. For type B, the high-pressure region covers almost the full section at the UT level. Therefore, the body may experience smoother support compared to type A. Besides, type A decreases the load on the head, which can help relieve the internal forces provided by the neck muscles. From a practical perspective, type B's headrest covers the whole width of the seat. Although it is required to provide more load to the head, it can support the head at more postures, especially when the passenger tends to lean laterally.

Conclusion

A parameterized model for an aircraft seat has been developed. Two types of designs with different headrest widths are analyzed regarding how the backrest sustains the head-cervical-thoracic region's bodyweight at different recline angles. This region of the body is presented by eight rigid segments. The assumed sitting postures are obtained, and the contact loadings are calculated based on the developed 3D multibody model. It is observed that type A backrest provides additional support on the upper thoracic region but reduces the loads required for the head support. However, the pressure distribution on type A is more partitioned, concentrated on two sides at the top area, which may round the upper trunk and cause discomfort. Type B has a smaller gradient of pressure change and can provide a wider range of support on the head.

References

Cappetti, N., & DI Manso, E. (2020). Study of the relationships between articular moments, comfort and human posture on a chair. *Work*, *68*, 1–10.

Drerup, B., & Hierholzer, E. (1994). Back shape measurement using video rasterstereography and three-dimensional reconstruction of spinal shape. *Clinical Biomechanics*, *9*(1), 28–36.

Du, X., Ren, J., Sang, C., & Li, L. (2013). Simulation of the interaction between driver and seat. *Chinese Journal of Mechanical Engineering (English Edition)*, *26*(6), 1234–1242.

Franz, M., Durt, A., Zenk, R., & Desmet, P. M. A. (2012). Comfort effects of a new car headrest with neck support. *Applied Ergonomics*, *43*(2), 336–343.

Harrison, C. R., & M, R. K. (2002). *CAESAR：Summary Statistics for the Adult Population (age 18 - 65) of USA*.

Kitazaki, S., & Griffin, M. J. (1997). A modal analysis of whole-body vertical vibration, using a finite element model of the human body. *Journal of Sound and Vibration*, *200*(1), 83–103.

Lim, S., Chung, M. K., Jung, J., & Na, S. H. (2000). The effect of lumbar support prominence on driver’s comfort and body pressure distribution. *Proceedings of the XIVth Triennial Congress of the International Ergonomics Association and 44th Annual Meeting of the Human Factors and Ergonomics Association, “Ergonomics for the New Millennium,”* 308–311.

Liu, Y. S., Zhong, X., Ghebreiyesus, W., Ji, J., & Xi, F. J. (2021). Analysis and modeling of human seat interaction with a focus on the upper body and backrest using biomechanics and contact mechanics. *Work*, *68*(s1), S161–S182.

Makhsous, M., Lin, F., Bankard, J., Hendrix, R. W., Hepler, M., & Press, J. (2009). Biomechanical effects of sitting with adjustable ischial and lumbar support on occupational low back pain: Evaluation of sitting load and back muscle activity. *BMC Musculoskeletal Disorders*, *10*, 1–

Paul, G., Pendlebury, J., & Miller, J. (2012). The contribution of seat components to seat hardness and the interface between human occupant and a driver seat. *International Journal of Human Factors Modelling and Simulation*, *3*(3/4), 378.

Pearsall, D. J., Reid, J. G., & Livingston, L. A. (1996). Segmental inertial parameters of the human trunk as determined from computed tomography. *Annals of Biomedical Engineering*, *24*(2),

Smulders, M., Naddeo, A., Cappetti, N., van Grondelle, E. D., Schultheis, U., & Vink, P. (2019). Neck posture and muscle activity in a reclined business class aircraft seat watching IFE with and without head support. *Applied Ergonomics*, *79*(April), 25–37.

White, A. A., & Panjabi, M. M. (1990). *Clinical Biomechanics of the Spine* (D. B. Cooke, D. PaUerson, G. Thrner, & K. Crown (eds.); second edi). Lippincott Williams & Wilkins.